NATIONAL ADVISORY COMMITTEE FOR AERONAUTICS

TECHNICAL MEMORANDUM

No. 1120

THE LIFT DISTRIBUTION OF SWEPT-BACK WINGS

By J. Weissinger

Translation

Uber die Auftriebsverteilung von Pfeilflugeln

Forschungsbericht Nr. 1553

Washington

March 1947

NATIONAL ADVISORY COMMITTEE FOR AERONAUTICS

TECHNICAL MEMORANDUM NO. 1120

THE LIFT DISTRIBUTION OF SWEPT-BACK WINGS*

By J. Weissinger

SYNOPSIS

Two procedures for calculating the lift distribution along the span are given, in which better account is taken of the distribution of circulation over the area than in the Prandtl lifting-line theory. The methods are also applicable to wings with sweepback. Calculated results according to two methods agree excellently. Using the second more simple method, one needs about 3 hours for the calculation of the lift distribution of a straight wing, and about 8 hours for this calculation for the swept-back wing. The results are compared with those of the Multhopp method and with experimental results. Finally, there is a brief note on the swept-back wing in sideslip.

TABLE OF CONTENTS

---

*"Über die Auftriebsverteilung von Pfeilflügeln," Zentrale für wissenschaftliches Berichtswesen der Luftfahrtforschung des Generalluftzeugmeisters (ZWB) Berlin-Adlershof. Forschungsbericht Nr. 1553. Berlin-Adlershof, den 27.2.1942.

INTRODUCTION

In the present report two methods for determining the lift distribution along the span are described, by means of which the influence of the wing plan form is taken into account better than by previous lifting-line theory. Since the new methods are also applicable to wings with sweepback, they represent an extension of previous theory, at least so far as scope of applicability is concerned.

The method described in the first section is based on the assumption of a lifting surface, and therefore will be designated as the "lifting-surface method," or "F-method." For a straight rectangular wing, the amount of calculation required is not materially greater than for known methods already in use; it gives a noticeably smaller $\frac{dc_a}{d\alpha}$ than the older methods, and this decrease of lift curve slope increases with decreasing aspect ratio Λ and amounts to approximately 8 percent for $\Lambda = 5$. Practically, this fact will be especially important for unsymmetrical lift distributions; for instance, one can deduce from it a noteworthy decrease of the rolling moment due to sideslip resulting from dihedral. In the general case of trapezoidal wings with and without sweepback, the required amount of calculation is quite considerable, and consequently one would only use the method in special instances for the control of the results from the more simple approximate method (L-method).

The method of the second section is based on a slightly modified model of previous lifting line theory, and hence will be designated as the "lifting-line method" or the "L-method." In spite of the radical simplification of the basic geometrical model compared to that of the F-method (and, consequently, in spite of the marked reduction of the required amount of calculation for trapezoidal and swept-back wings), the results show an excellent agreement with those of the first method.

In the third section the results obtained with the new methods (the calculations have been subjected to numerous checks, but have not been carried out twice independently) are discussed, and compared with experiment. In addition, a comparison is made with the Multhopp method

of calculating swept-back wings (10). The note on the rolling moment due to sideslip of swept-back wings contained in the fourth section is actually outside the scope of the present report, which, except for this note, is concerned with symmetrical flow incidence, but is made here in order to quickly remove a widespread misconception.

In this interim report, intended to make available to practice as quickly as possible the results obtained to date, the F-method is only described in detail for the straight rectangular wing, and the detailed application of it for general wings is not given, especially since these mathematical details are of less interest to the practical aerodynamicist. These matters together with some supplementary material will be included in a later report.

NOTATION

x, y or ξ, η — coordinates in vortex plane (See fig. 1(a).)

$\bar{x} = \frac{x}{t/2}$, $\bar{\xi} = \frac{\xi}{t/2}$

$\bar{y} = \frac{y}{b/2}$, $\bar{\eta} = \frac{\eta}{b/2}$ — dimensionless coordinates

F — wing area

b — wing span

t — wing chord

$\Lambda = \frac{b^2}{F}$ — aspect ratio

$\lambda(\bar{y}) = \frac{b}{t(\bar{y})}$ — local aspect ratio

Z — taper ratio (ratio of root chord to tip chord)

φ — sweepback angle (measured at $\frac{1}{4}$ chord line)

α — angle of attack

β angle of sideslip

v incident flow velocity

c_a lift coefficient $\left(A = c_a \frac{\rho}{2} v^2 F\right)$

c_m pitching-moment coefficient $\left(M = c_m \frac{\rho}{2} v^2 F \frac{F}{b}\right)$

c_L rolling-moment coefficient $\left(L = c_L \frac{\rho}{2} v^2 F \frac{b}{2}\right)$

a distance of the center of lift of a wing half from the plane of symmetry of the wing referred to the semispan.

$\gamma(x,y)$ circulation density of the bound vortex

$\Gamma(y)$ circulation distribution along the span

$G(\overline{y}) = \frac{\Gamma(\overline{y})}{b\ v}$ dimensionless circulation distribution

$F(l)$, $\overline{F}(l)$ influence functions for F-method

$L(l)$ influence function for L-method

$l = \lambda(\overline{y} - \overline{\eta})$ argument of influence functions

I. THE LIFTING SURFACE METHOD (F-METHOD)

As remarked in the introduction, this method will only be derived here for the simplest case of the straight rectangular wing. If such a wing is replaced by a plane system of vortices (see fig. 1(a)), in the sense of customary lifting surface theory (see for example Blenk (2)), and if one denotes the density of circulation of the bound vortices by $\gamma(\xi, \eta)$ the induced velocity of the point x,y may be calculated as

$$w_A(x,y) = \int_{-t/2}^{+t/2} \int_{-b/2}^{+b/2} \left[\frac{1}{\overline{y} - \overline{\eta}} + \frac{\sqrt{(x-\xi)^2 + (y-\eta)^2}}{(x-\xi)(y-\eta)} \right] \frac{\partial \gamma(\xi, \eta)}{\partial \eta} \, d\xi \, d\eta \qquad (1)$$

By taking into account the two equations

$$\int_{-t/2}^{t/2} \gamma(\xi,\eta)d\xi = \Gamma(\eta) = \text{circulation at a wing section} \quad (2)$$

$$\int_{-b/2}^{b/2} \frac{\sqrt{(y-\eta)^2}}{y-\eta} \frac{\partial\gamma(\xi,\eta)}{\partial\eta} d\eta = 2\gamma(\xi,y) \quad (3)$$

one can write instead

$$\boxed{w_A(x,y) = \frac{1}{4\pi}\int_{-b/2}^{b/2} \frac{\Gamma'(\eta)}{y-\eta} d\eta + \frac{1}{2\pi}\int_{-t/2}^{t/2} \frac{\gamma(\xi,y)}{x-\xi} d\xi}$$

$$+ \frac{1}{4\pi}\int_{-b/2}^{b/2}\int_{-t/2}^{t/2} \frac{\sqrt{(x-\xi)^2+(y-\eta)^2} - \sqrt{(y-\eta)^2}}{(x-\xi)(y-\eta)} \frac{\partial\gamma(\xi,\eta)}{\partial\eta} d\xi\, d\eta \quad (4)$$

$\gamma(\xi,\eta)$ is to be determined by the requirement that $w_A(x,y)$ shall be equal to the prescribed normal component $V_n(x,y)$ of the incident flow velocity at the wing. If one only takes into account the part enclosed in frame $w_A(x,y)$ the condition is

$$\frac{1}{2\pi}\int_{-t/2}^{t/2} \frac{\gamma(\xi,y)}{x-\xi} d\xi = V_n(x,y) - \frac{1}{4\pi}\int_{-b/2}^{b/2} \frac{\Gamma'(\eta)}{y-\eta} d\eta \quad (5)$$

This is the equation of the two-dimensional problem for the profile section located at the station y having the normal-component distribution given on the right hand side of the equation. If $V_n(x,y)$ is independent of x one may obtain from the two-dimensional theory the solution

$$\gamma(\xi,y) = \frac{2}{\pi t}\sqrt{\frac{\frac{t}{2}-\xi}{\frac{t}{2}+\xi}}\cdot\Gamma(y) \qquad (6)$$

$$\Gamma(y) = \pi t\left[V_n(y) - \frac{1}{4\pi}\int_{-b/2}^{b/2}\frac{\Gamma'(\eta)}{y-\eta}\,d\eta\right] \qquad (7)$$

in which the second relation is obviously identical with the Prandtl lifting line equation for the determination of $\Gamma(y)$. According to Pistolesi (11) this relation is also valid approximately for normal-component distributions which are dependent on x. If for $V_n(y)$ one substitutes the value of the normal component at the three-quarter point (Multhopp (10) has pointed out the importance of this idea, which seems to have been almost universally forgotten, for numerous applications), the approximation is rigorously correct if the dependence on x is linear, that is to say, the same as it is for a circular-arc profile.

Since the term of $W_A(x,y)$ not enclosed in the frame vanishes for $\Lambda \to \infty$ (for, as is proved in (14) the equation for the lifting surface goes into equation (5) for $\Lambda \to \infty$), and also since it is known that the Prandtl equation is in good agreement with experiment down to $\Lambda = 4$, this part may be regarded as a correction term to the Prandtl equation, and since it is a correction term it need be taken into account only approximately. In order to arrive at an equation for the determination of $\Gamma(\eta)$ which will be similar to the Prandtl equation, one must first of all get rid of the dependence on x in the term in question, and this is done by Pistolesi's approximation by replacing it by its value at the three-quarter chord point (that is, $x = \frac{t}{4}$), and in the second place $\gamma(\xi,\eta)$ must be prescribed as a function of ξ for which the most suitable approximation is equation (6). One may easily convince himself that the same result will be obtained by incorporating both of these procedures in the initial equation (1). The following equation is then obtained:

$$V_n = \frac{1}{4\pi}\int_{-b/2}^{b/2} \frac{\Gamma'(\eta)}{y-\eta}\,d\eta$$

$$+ \frac{1}{2\pi^2 t}\int_{-b/2}^{b/2}\int_{-t/2}^{t/2} \frac{\sqrt{(x-\xi)^2 + (y-\eta)^2}}{(x-\xi)\quad(y-\eta)} \sqrt{\frac{\frac{t}{2}-\xi}{\frac{t}{2}+\xi}}\;\Gamma'(\eta)\,d\xi\,d\eta \qquad (8)$$

in which x is to be set equal to $\frac{t}{4}$.

By introducing dimensionless quantities,

$$\left.\begin{aligned} y = \frac{b}{2}\bar{y},\ \eta = \frac{b}{2}\bar{\eta},\ x = \frac{t}{2}\bar{x},\ \xi = \frac{t}{2}\bar{\xi} \\ \Gamma(\eta) \equiv b\,V\,G(\eta),\ a = \frac{V_n}{V} \end{aligned}\right\} \qquad (9)$$

we obtain

$$a = \frac{1}{2\pi}\int_{-1}^{1} \frac{G'(\bar{\eta})}{\bar{y}-\bar{\eta}}\,d\bar{\eta}$$

$$+ \frac{1}{2\pi^2}\int_{-1}^{1}\int_{-1}^{1} \frac{\sqrt{(\bar{x}-\bar{\xi}) + \Lambda^2(\bar{y}-\bar{\eta})^2}}{(\bar{x}-\bar{\xi})(\bar{y}-\bar{\eta})} \sqrt{\frac{1-\bar{\xi}}{1+\bar{\xi}}}\;G'(\bar{\eta})\,d\bar{\xi}\,d\bar{\eta} \qquad (10)$$

where $\bar{x} = 0.5$. If for abbreviation, we set

$$F^*\left[\Lambda(\bar{y}-\bar{\eta})\right] = \frac{1}{\pi}\int_{-1}^{1} \frac{\sqrt{(\bar{x}-\bar{\xi})^2 + \Lambda^2(\bar{y}-\bar{\eta})^2}}{\bar{x}-\bar{\xi}} \sqrt{\frac{1-\bar{\xi}}{1+\bar{\xi}}}\,d\bar{\xi} \qquad (11)$$

$$F_o^* = F^*\left[\Lambda(\bar{y} - \bar{\eta})\right]_{\bar{\eta}=\bar{y}} = \frac{2}{\pi}\left(\arcsin \bar{x} + \sqrt{1 - \bar{x}^2}\right) \qquad (12)$$

$$F\left[\Lambda(\bar{y} - \bar{\eta})\right] = \frac{F^*\left[\Lambda(\bar{y} - \bar{\eta})\right] - F_o^*}{\Lambda(\bar{y} - \bar{\eta})} = F(\zeta), \quad \zeta = \Lambda(\bar{y} - \bar{\eta}) \qquad (13)$$

equation 10 becomes

$$\alpha = \frac{1 + F_o^*}{2\pi}\int_{-1}^{+1} \frac{G'(\bar{\eta})}{\bar{y} - \bar{\eta}}\, d\bar{\eta} + \frac{\Lambda}{2\pi}\int_{-1}^{+1} F\left[\Lambda(\bar{y} - \bar{\eta})\right] G'(\bar{\eta})\, d\bar{\eta} \qquad (14)$$

where $F_o^* = 0.8847$ corresponding to $\bar{x} = 0.5$.

Since $F(\zeta)$ is continuous everywhere, the numerical evaluation of the last integral involves no fundamental difficulty. The function $F(\zeta)$ may be calculated with the help of elliptical integrals, but practically one would get the answer more quickly using numerical approximation methods. $F(\zeta)$ is an antisymmetrical function whose positive branch is shown in figure 2.

The solution of the integral differential equation (14) will be carried out in analogy to the Multhopp procedure (9), familiarity with which is here assumed, especially familiarty with the Multhopp notation (the Multhopp dimensionless circulation γ is designated here by G). To this end, we need a mechanical integration formula, the proof of which is analogous to that of the formula used by Multhopp (9), (10).

It is:

If $f(\bar{\eta})$ is a polynomial in $\bar{\eta}$ of degree $(2M + 1)$, that is, of the form

$$f(\bar{\eta}) = \sum_{\upsilon=0}^{2M+1} C_\upsilon \bar{\eta}^\upsilon = \sum_{\upsilon=0}^{2M+1} C_\upsilon \cos \upsilon\psi \qquad (15)$$

then we have without any approximation:

$$\int_{-1}^{1} \frac{f(\bar{\eta})}{\sqrt{1 - \bar{\eta}^2}}\, d\bar{\eta} = \frac{\pi}{M + 1}\left[\frac{f(-1) + f(+1)}{2} + \sum_{n=1}^{M} f(\bar{\eta}_n)\right] \qquad (16)$$

or writing $\psi = \cos^{-1} \bar{\eta}$

$$\int_0^{\pi} f(\psi)d\psi = \frac{\pi}{M+1}\left[\frac{f(\psi_0) + f(\psi_{M+1})}{2} + \sum_{n=1}^{M} f(\psi_n)\right] \qquad (17)$$

where

$$\psi_\eta = n\frac{\pi}{M+1}$$

According to the Multhopp substitution

$$G(\psi) = \frac{2}{m+1}\sum_{n=1}^{m} G_n \sum_{\mu=1}^{m} \sin \mu\vartheta_n \sin \mu\psi \qquad (18)$$

and using

$$f_n(\psi) = \frac{2}{m+1}\sum_{\mu=1}^{m} \mu \sin \mu\vartheta_n \cos \mu\psi \qquad (19)$$

one obtains for $G'(\psi)$ the form

$$G'(\psi) = \sum_{n=1}^{m} G_n f_n(\psi) \qquad (20)$$

If this expression is substituted in the second integral of (14) one gets the following approximation from the mechanical integration formula:

$$\frac{1}{2\pi}\int_{-1}^{1} F\left[\Lambda(\bar{y}_\upsilon - \bar{\eta})\right] G'(\bar{\eta})\, d\bar{\eta} = \sum_{n=1}^{m} \bar{g}_{\upsilon n} G_n \qquad (21)$$

where $g_{\upsilon n} = -\frac{1}{2\pi}\int_0^{\pi} F\left[\Lambda(\bar{y}_\upsilon - \bar{\eta})\right] f_n(\psi)\, d\psi$

$$= -\frac{1}{2(M+1)}\left(\frac{f_{no} F_{\upsilon o} + f_{n,M+1} F_{\upsilon,M+1}}{2} + \sum_{\mu=1}^{M} f_{n\mu} F_{\upsilon\mu}\right) \qquad (22)$$

in which for the sake of simplicity we have written

$$f_{n\mu} = f_n(\psi_\mu), \quad F_{\upsilon\mu} = F\left[\Lambda(\bar{y}_\upsilon - \bar{\eta}_\mu)\right], \quad \bar{\eta}_\mu = \arccos \psi_\mu \tag{23}$$

By taking into account the Multhopp quadrature formula for the first integral, one now obtains from equation (14) the following system of linear equations for the determination of the G_υ:

$$b_\upsilon^* G_\upsilon = a_\upsilon + \sum_{n=1}^{m}{}' b_{\upsilon n}^* G_n, \quad \upsilon = 1, 2, \ldots, m \tag{24}$$

where

$$b_\upsilon^* = (1 + F_o^*)b_{\upsilon\upsilon} + \Lambda g_{\upsilon\upsilon}, \quad b_{\upsilon n}^* = (1 + F_o^*)b_{\upsilon n} - \Lambda g_{\upsilon n} \tag{25}$$

For symmetrical circulation distributions these equations are further simplified to

$$B_\upsilon^* G_\upsilon = a_\upsilon + \sum_{n=1}^{\frac{m+1}{2}}{}' B_{\upsilon n}^* G_n, \quad \upsilon = 1,2,\ldots,\frac{m+1}{2} \tag{26}$$

where

$$B_\upsilon^* = (1 + F_o^*)b_{\upsilon\upsilon} + \Lambda \bar{g}_{\upsilon\upsilon}, \quad B_{\upsilon\eta}^* = (1 + F_o^*)B_{\upsilon n} - \Lambda \bar{g}_{\upsilon n} \tag{27}$$

and

$$\bar{g}_{\upsilon n} = \frac{-1}{2(M+1)} \sum_{\mu=o}^{\frac{M-1}{2}} \bar{F}_{n\mu}(F_{\upsilon\mu} - F_{\upsilon\bar{\mu}}), \quad \bar{\mu} = M + 1 - \mu \tag{28}$$

The $\bar{F}_{n\mu}$ which appear here are formed from the $f_{n\mu}$ and are given in table I for $m = 7$ and $M = 7$, 15, 31 and in table II for $m = 15$ and $M = 15$. Their calculation was not made with formulas (19), but, in particular for the case $m = M$ in a considerably simpler manner to which, however, no further reference will be made here.

The method of calculation of the lift distribution of a straight rectangular wing with symmetrical angle of attack distribution is, then, for the case $m = 7$ as follows:

According to the degree of accuracy required, one chooses a certain M, multiplies the differences $(\cos\theta_\nu - \cos\theta_\mu)$ found in table III with the aspect ratio Λ, then reads for the points $l_{\nu\mu} = \Lambda(\cos\theta_\nu - \cos\theta_\mu)$ the values $F_{\nu\mu}$ of the function $F(l)$ from figure 2[1] then forms the difference $F_{\nu\mu} - F_{\nu\bar{\mu}}$ and with them using table I the product sums $\sum_{\mu=0}^{\frac{M+1}{2}} F_{n\mu}(F_{\nu\mu} - F_{\nu\bar{\mu}})$, which can be done on a calculating machine without very much trouble. By multiplication with $-\Lambda/2(m+1)$ one obtains from them the quantities $\Lambda\bar{g}_{\nu n}$ and from them the Multhopp coefficients $B_{\nu n}$, $b_{\nu\nu}$ according to formula (27) and also the coefficients B_ν^*, $B_{\nu n}^*$ of the system of linear equations (26) which may be solved by the Multhopp iteration procedure. In doing this it is to be noted that half of the coefficients do not vanish as in the case of the Multhopp calculations.

In the case $M = m$ for which most of the $l_{\nu\mu}$ and consequently also the $F_{\nu\bar{\mu}}$ are equal but of opposite sign, one needs for $m = 7$ about 3 hours for the calculation of a lift distribution. For constant angle of attack over the span, the accuracy obtained by setting $M = m$ is always sufficient, at any rate for $0 \leq \Lambda \leq 10$ although the quantities $\bar{g}_{\nu n}$ do not come out very accurately. They are, however, partly too large and partly too small, so that the lift distribution is hardly affected: for instance, for $\Lambda = 5$, $\alpha = 1$, $m = 7$ in the calculation to 3 decimals there was no distinction between the cases $M = 7$, $M = 15$, and $M = 31$. The increase of accuracy resulting from the choice of a larger m corresponds to that of the Multhopp method.

The Pistolesi approximation is rigorously correct for normal-component distribution of the form $V_n = c_o + c_1 \cos\varphi$ where $\varphi = \cos^{-1}\bar{x}$. If the third term of the Fourier development is also to be considered, the value to be taken for V_n is not the value at the three-quarter chord point, but the mean of the values at the center of the profile and at the trailing edge. In order to introduce this approximation into the above calculation, one must regard $\bar{x}$ as not yet nailed down to a definite numerical

[1] In order to improve the accuracy of reading the values, a curve with doubled scale was used.

value, and hence $F^*(l)$ and $F(l)$ are regarded as functions: $F^*(l,\bar{x})$, $F(l,\bar{x})$ of $\bar{x}$: with these one forms

$$\left.\begin{aligned} \bar{F}(l) &= \frac{F(l,0) + F(l,1)}{2} \\ \text{and} \qquad \bar{F}_o^* &= \frac{F_o^*(0) + F_o^*(1)}{2} \end{aligned}\right\} \tag{29}$$

and one obtains the equation

$$\alpha = \frac{1 + \bar{F}_o^*}{2\pi} \int_{-1}^{1} \frac{G'(\bar{\eta})}{\bar{y} - \bar{\eta}}\, d\bar{\eta} + \frac{\Lambda}{2\pi} \int_{-1}^{1} \bar{F}\left[\Lambda(\bar{y} - \bar{\eta})\right] G'(\bar{\eta})\, d\bar{\eta} \tag{30}$$

The course of the calculation is the same as for equation (14) if one replaces F by $\bar{F}$ and F_o^* by $\bar{F}_o^* = 0.8183$ everywhere. The function $\bar{F}(l)$ is likewise plotted in figure 2.

A comparison made for a case with $\Lambda = 5$ shows that taking into account the second Pistolesi approximation as well as the first does not give anything, at least for the degree of accuracy employed in the calculation; c_a changes by 0.5 percent. Since, however, after $\bar{F}(l)$ is once calculated, the amount of calculation in the two cases is the same; the systematic calculations for the straight rectangular wing were carried out with the function $\bar{F}$ ($\bar{F}$-method). For a number of aspect ratios between 0 and 10 the lift distributions were calculated on the one hand by the Prandtl lifting-line equation, and on the other hand by equation (30); three examples are given in figure 3. For large Λ a difference is perceptible only at the wing tip where the influence of induction is greatest; with decreasing Λ the difference becomes greater, and is in evidence over more and more of the span. The new distribution always lies under the old, since induction now comes into play more strongly. In addition, the corresponding lift coefficients were determined and compared with the old values. As $\Lambda \to 0$ the ratio $\frac{1}{1 + \bar{F}_o^*}$ tends toward the value 0.55. But even in the

range of normal aspect ratios, the deviations are always noticeable, as may be seen from figure 4. For purposes of comparison, some points for the elliptical wing calculated by Helmbold are also included (the distinction between rectangle and ellipse for very small Λ which is revealed here is caused by the difference of the basic vortex systems). According to the L-method discussed in II we also have for the rectangular wing the limit 0.5 as $\Lambda \to 0$. From this figure one can also take a correction for the old formulas used to recalculate to a different aspect ratio, which correction to be sure ordinarily does not amount to very much.

The new method will give significant differences for antisymmetrical angle of attack distributions. Although calculations for such cases are not available, certain conclusions may be drawn from figure 4. For an antisymmetrical lift distribution the lift of a wing-half will behave with respect to the induction effect approximately like a wing with half the span; that is, the lift of a wing-half calculated as formerly and the corresponding rolling moment are to be multiplied by the ratio $\frac{c'_{aF}}{c'_{aP}}$ read from figure 5 at the point $\frac{\Lambda}{2}$. Thus the rolling moment due to sideslip caused by dihedral for a rectangular wing with aspect ratio = 5 would have to be about 15 percent less than previously calculated, and actually Moeller (8) measured a moment 18 percent too small according to the then existing theory.

When the method is extended to swept-back wings, a number of new difficulties arises, which brings about a complication of the formulas and with it an increase of the computational work. For this reason, the explanation of the general procedure will not be given in this interim report. For this calculation the basis would be the vortex system of the lifting surface as it is shown in the example of figure 1(b). The difficulty caused by the induced velocity becoming infinite at the center of the wing is overcome by splitting up; that is, the circulation distribution $G(\bar{\eta})$ is substituted in the form $G(\bar{\eta}) = \bar{G}(\bar{\eta}) + C|\bar{\eta}|\sqrt{1 - \bar{\eta}^2}$ with a suitable constant C or, expressing this in physical terms, the singularity of the induced velocity caused by the bound

vortices is neutralized by the free vortices. In this way we also accomplish something else at the same time, namely that the distribution $\overline{G}(\overline{\eta})$ which is what we are solving for, and which is approximated by a Multhopp Fourier expression, looks like the distribution of the straight wing, so that it can be determined quite accurately, even for large sweep angles, with $m = 7$. (See fig. 5.) The calculation was carried out for rectangular wings, $\Lambda = 5$ with sweep angles $\varphi = 0^\circ, 15^\circ, 45^\circ$; the result is shown in figure 6. The purpose of these curves is to serve as a basis of comparison with the lifting line method which will now be described.

II. THE LIFTING-LINE METHOD (L-METHOD)

Given a wing with a straight one-quarter chord line, think of the usual model of the lifting line so situated at the wing that the lifting line is situated at the one-quarter chord line (see fig. 7(a)) and then determine (with reference to Pistolesi's approximation) the circulation distribution, so that the vertical component of the induced velocity due to this vortex system at the three-quarter chord line is equal and opposite to the corresponding component of the incident flow (to my knowledge, this model was first used by Wieghardt (16), page 261/262 in a special form). One has a right to expect that the influence of the free vortices is pretty well taken into account by this simplified model, since, although they are shorter than the ones on the lifting surface, they are of constant density and do not decrease to zero, as on the lifting surface. With reference to the bound vortices, it will now be helpful that in the case of the infinitely wide plane plate the downwash of the lifting surface and the downwash of the lifting line located at the one-quarter chord position are equal to each other at the three-quarter chord distance. (This result is taken from a work by Helmbold which is not yet published.)

At the general point (x,y) in the plane of the vortex sheet the lifting-line model induces the following down draft velocity:

$$w_A(x,y) = \frac{1}{4\pi} \int_{-b/2}^{b/2} \frac{1}{y - \eta} \left[1 + \frac{1}{x} \sqrt{x^2 + (y - \eta)^2} \right] \Gamma'(\eta)\, d\eta \quad (31)$$

and if one introduces here the dimensionless notation of (9) and also writes $\lambda = \frac{b}{t(\bar{y})}$ and $x = \frac{t(\bar{y})}{2}$ this becomes

$$\frac{w_A}{V} = \frac{1}{2\pi}\int_{-1}^{1} \frac{1}{\bar{y} - \bar{\eta}} \left[1 + \sqrt{1 + \lambda^2(\bar{y} - \bar{\eta})^2}\right] G'(\bar{\eta})\, d\bar{\eta} \qquad (32)$$

Introducing the notation

$$L\left[\lambda(\bar{y} - \bar{\eta})\right] = \frac{\sqrt{1 + \lambda^2(\bar{y} - \bar{\eta})^2} - 1}{\lambda(\bar{y} - \bar{\eta})} \qquad (33)$$

we obtain the following equation for the determination of $G(\bar{\eta})$:

$$\alpha = \frac{2}{2\pi}\int_{-1}^{1} \frac{G'(\bar{\eta})}{\bar{y} - \bar{\eta}}\, d\bar{\eta} + \frac{\lambda}{2\pi}\int_{-1}^{1} L\left[\lambda(\bar{y} - \bar{\eta})\right] G'(\bar{\eta})\, d\bar{\eta} \qquad (34)$$

This equation obviously has the same form as equation (14) or (30) for the lifting-surface method. Consequently the numerical treatment is according to the same scheme as given on pages 10/11, except that there F_o^* is replaced by 1, F is replaced by L and Λ by $\lambda_v = \frac{b}{t_v}$. The antisymmetric function $L(l)$ is to be taken from figure 8.

The application of the model to swept-back wings makes no difficulty (compare fig. 7(b)), since there are no singularities of the induced velocity at the three-quarter chord line. For the down-draft velocity at a point (x,y) we have for $y \geqq 0$

$$w_A(x,y) = \frac{1}{4\pi}\int_{-b/2}^{b/2} \frac{\Gamma'(\eta)}{y-\eta}\left[1 + \frac{x - |\eta| \tan\varphi}{\sqrt{(x - |\eta| \tan\varphi)^2 + (y-\eta)^2}}\right] d\eta$$

$$+ \frac{1}{4\pi}\int_{-b/2}^{0} \Gamma(\eta) \frac{x + y\tan\varphi}{\sqrt{(x - |\eta| \tan\varphi)^2 + (y-\eta)^2}^3}\, d\eta$$

$$+ \frac{1}{4\pi}\int_{0}^{b/2} \Gamma(\eta) \frac{x - y\tan\varphi}{\sqrt{(x - |\eta| \tan\varphi)^2 + (y-\eta)^2}^3}\, d\eta \qquad (35)$$

The last two integrals represent the induced velocity of the lifting line, and after integrating them by parts one obtains

$$w_A = \frac{1}{4\pi}\int_{-b/2}^{0} \left\{\frac{1}{y-\eta}\left[1 + \frac{\sqrt{(x - |\eta| \tan\varphi)^2 + (y-\eta)^2}}{x + y\tan\varphi}\right]\right.$$

$$\left. + 2\tan\varphi \frac{\sqrt{x^2 + y^2}}{x^2 - y^2\tan^2\varphi}\right\}\Gamma'(\eta)\, d\eta$$

$$+ \frac{1}{4\pi}\int_{0}^{b/2}\left[1 + \frac{\sqrt{(x - |\eta| \tan\varphi)^2 + (y-\eta)^2}}{x - y\tan\varphi}\right]\frac{\Gamma'(\eta)}{y-\eta}\, d\eta \qquad (36)$$

If now one again chooses the point at which the downwash is computed at the three-quarter chord distance, or in other words, $x = y\tan\varphi + \frac{t(y)}{2}$ and if one introduces dimensionless notation, and also the function

$$L_\varphi(\bar{y},\bar{\eta}) = \begin{cases} \dfrac{1}{\lambda(\bar{y}-\bar{\eta})}\left[\dfrac{\sqrt{[1+\lambda\tan\varphi\,(\bar{y}-|\bar{\eta}|)]^2+\lambda^2(\bar{y}-\bar{\eta})^2}}{1+2\lambda\tan\varphi\,\bar{y}}-1\right] \\ \quad + 2\tan\varphi\,\dfrac{\sqrt{[1+\lambda\tan\varphi\,\bar{y}]^2-\lambda^2\bar{y}^2}}{1+2\lambda\tan\varphi\,\bar{y}}\,;\ \bar{\eta}\leq 0 \qquad (37) \\ \dfrac{\sqrt{[1+\lambda\tan\varphi(\bar{y}-|\bar{\eta}|)]^2+\lambda^2(\bar{y}-\bar{\eta})^2}-1}{\lambda(\bar{y}-\bar{\eta})},\quad \bar{\eta}\geq 0 \end{cases}$$

one obtains the following equation for the determination of $G(\bar{\eta})$

$$\alpha = \frac{2}{2\pi}\int_{-1}^{1}\frac{G'(\bar{\eta})}{\bar{y}-\bar{\eta}}\,d\bar{\eta} + \frac{\lambda}{2\pi}\int_{-1}^{1}L_\varphi\,(\bar{y},\bar{\eta})\;G'(\bar{\eta})\;d\bar{\eta} \qquad (38)$$

which may be solved by the same method as the earlier equations since $L_\varphi(\bar{y},\bar{\eta})$ is continuous. Compared with the case of no sweepback, the computational work is more tedious because the function $L_\varphi(\bar{y},\bar{\eta})$ is not a universal function of $\lambda(\bar{y}-\bar{\eta})$ as in the case $\varphi = 0^\circ$; instead the values $L_\varphi(\bar{y}_\upsilon,\bar{\eta}_\mu)$ must be calculated afresh for every Λ, t, φ. If one writes $L_\varphi(\bar{y},\bar{\eta})$ as a function of $\lambda(\bar{y}-\bar{\eta})$ one gets a different function for each point at which the downwash is computed, $\bar{y}$, for instance if $m = 7$, four different functions. In figure 6 the results of calculations by the F-method and by the L-method are given for a rectangular wing of aspect ratio $A = 5$ with sweep angles $\varphi = 0^\circ, 15^\circ, 45^\circ$. The agreement is very good. If, on the basis of these examples, which to be sure should perhaps be increased, one assumes a general agreement of the two methods, one may in the future use only the less laborious L-method. In contrast to the Multhopp method (compare section III and also figures 11, 12) the convergence of the L-method is also very good for large sweep angles; an increase in the number of points from $m = 7$ to $m = 15$ does not effect any essential change, as may be seen from figure 6. For the same reason

as in the case of the straight rectangular wing (see p. 11) one may also calculate $\bar{g}_{\nu n}$ for the pointed and swept-back wing by taking $M = m$ points. Using $m = M = 7$ one needs about 8 hours for the calculation of the lift distribution of the swept-back wing.

III. NUMERICAL RESULTS COMPARISON WITH THE MULTHOPP METHOD AND WITH THE RESULTS OF EXPERIMENT

In figures 9 and 10 the results of the calculation for a rectangular wing of $\Lambda = 5$ and for a trapezoidal wing of $\Lambda = 5$, and $Z = 2$ and different sweep angles are plotted. For comparison the curves calculated by the Multhopp method (10) for $\varphi = 0°$ and $\varphi = 45°$ and with $K = 1$ and $m = 7$ are included. The large difference in total lift is particularly apparent. This may be explained as follows:

Multhopp assumed that the factor of proportionality between circulation and angle of attack was independent of angle of sweepback, because experiment showed, at least for sweep angles which were not too great, no effect of sweep on total lift. The present calculations, however, were primarily intended to give as good an approximation as possible to the rigorous theory of the lifting surface, in order that a solid foundation might be obtained for the estimation of various secondary effects such as boundary layer, tip vortices, etc. Theoretically, however, sweepback must cause a decrease of lift, as one may easily convince himself, and indeed by a factor of $\cos \varphi$ for the wing of infinite aspect ratio, while for finite aspect ratio as a result of the vortex sheet the decrease is not quite so large. Based on an approximate calculation which will not be given in detail here, the factor turns out to be $\frac{\Lambda + 2}{\frac{\Lambda}{\cos \varphi} + 2} \approx 1 - \frac{\varphi^2}{2} \times \frac{\Lambda}{\Lambda + 2}$. In table 5 the values $c_a' = \frac{dc_a}{d\alpha}$ together with their percentage deviations from c_a' for $\varphi = 0$ are given for the examples which were calculated. The deviations are given very well by the expression $\frac{\varphi^2}{2} \times \frac{\Lambda}{\Lambda + 2}$.

As a second difference between the two methods, one sees from figures 9 and 10 that according to the Multhopp distribution the lift is displaced a little more strongly toward the wing tips. Table VI gives the position of the center of lift $\frac{ab}{2}$ on the span according to the Multhopp formula (4.7),(10). From the same table one may take the difference Δa of the centers of lift for the swept-back wing and the straight wing, the magnitude of which is decisive for the question of whether the neutral point of the swept-back wing may or may not be calculated from the lift distribution of the straight wing. Referred to average wing chord $\frac{F}{b}$ the error is $\tan\varphi\, \Delta a \quad \frac{\Lambda}{2}$ a quantity which is likewise given in table VI. If a maximum error of 1 percent of the average chord is permissible, then at least theoretically one must use the lift distribution of the swept-back wing beyond $\varphi \approx 20°$. One sees, moreover, that for $\varphi = 45°$ the difference between the Multhopp method, and the lifting-line method is considerably greater than the permissible amount. For large sweep angles the error introduced by the integration formula (4.7),(10) also plays a role. In order to form an estimate of its magnitude, certain values of a were determined by planimetry of the corresponding integral areas, and are likewise given in table VI. Here again one gets deviations which are too large for $\varphi = 45°$.

In an attempt to explain the differences between the Multhopp method and the L-method, the convergence behavior of the Multhopp method was examined in certain numerical cases. Figure 11 shows one example (rectangle $\Lambda = 5, \varphi = 45°$). Multhopp himself points out that, on account of the divergence of his integral for w_A there would be no point in the case of $K = 1$ to increase the number of points m to more than 7. This is confirmed by calculation. The distribution calculated for $m = 15$ is very different from the one calculated for $m = 7$. Also when the correction function K (fig. 1 (10)) is used, there is a marked difference at the center of the wing when $m = 7$ and $m = 15$. (In this connection it may be said that all the equations of the F-method and of the L-method lead to the form

$$\alpha = \frac{1}{2\pi}\int_{-1}^{1} \frac{1}{\bar{y} - \bar{\eta}} \frac{\partial}{\partial\bar{\eta}} \left[G(\bar{\eta})\, H(\bar{y},\bar{\eta})\right] d\bar{\eta}$$

for suitable $H(\bar{y},\bar{\eta})$ from which, using the Multhopp method of integration, the following system of linear equations is obtained).

$$a_\upsilon = b_{\upsilon\upsilon} H_{\upsilon\upsilon} G_\upsilon - \sum_{n=1}^{m}{}' b_{\upsilon n} H_{\upsilon n} G_n , \quad \upsilon = 1,2, \ldots, m$$

This method is formally very simple, but converges frightfully slow: $m = 31$ is not even sufficient. If for the swept-back wing one calculates the term due to the sweep angle by this method, one has a method which is very similar to the Multhopp method for swept-back wing with $K = 1$, and also has the same convergence behavior. Very peculiarly, over the rest of the wing the difference between the most exact calculation ($m = 15$, $K = 1$) and the roughest calculation ($m = 7$, $K = 1$) is not excessively great. A similar result may be seen for the trapezoidal wing with $\Lambda = 5$, $Z = 2$, and $\varphi = 45^\circ$. (See fig. 12.) According to this, there does not seem to be much point in including the correction factor K in the Multhopp method.

The question of agreement between theory and experiment is difficult to answer, because at the present time there are not many measurements of swept-back wings available, and the accuracy of the ones which are available is not always sufficient. The following is based on the rectangular wing measurements by Blenk (3) ($\Lambda = 5$; $\varphi = 0^\circ, 15^\circ, 30^\circ$) and Hansen (4) ($\Lambda = 4.8$; $\varphi = -10^\circ, 0^\circ, 10^\circ, 20^\circ, 40^\circ$) on the trapezoidal wing measurements of the NACA (1) ($\Lambda = 6$; $Z = 2$; $\varphi = 0^\circ, 15^\circ, 30^\circ$) on a fairly recent series of observations of trapezoidal wings with $-35^\circ < \varphi < 45^\circ$, by Luetgebrune (6) (7) and on an unpublished DVL measurement of a trapezoidal wing with $\varphi = 0^\circ$ and $\varphi = 35^\circ$. Regarding the Multhopp thesis that $\frac{dc_a}{d\alpha}$ is not influenced by sweepback, this is certainly true for the interval of small sweep angles up to 15°, or more precisely it is not detectable since changes of $\frac{dc_a}{d\alpha}$ by 2 percent or 3 percent which would be expected from the L-method for $\varphi = 15^\circ$ are hardly perceptible experimentally, especially since the $c_a(\alpha)$ curve is generally not entirely straight; but this

assertion is also made by Luetgebrune (6) for large sweep angles on the basis of his measurements. In my opinion, however, these measurements cannot be used to decide the matter, since the dispersion (explained by inaccuracies of the model) of the measured c_a' values about the mean which was supposed to be independent of φ was almost ± 10 percent (see fig. 9 '6)), so that the errors here were about as great as the difference in question. Similarly the VDT measurement (1) cannot be used, particularly because the corrections to that cannot be checked. If one attempts to interpolate the Blenk values of $c_a(\alpha)$ by a straight line, one gets for $\varphi = 30°$ a decrease of c_a' by about 6 percent compared to $\varphi = 0°$, while from table V one can take 10.7 percent. The DVL measurement ($\Lambda \sim 5.7$, $Z \sim 1.9$) shows for $\varphi = 35°$ a decrease of about 8 percent, while the theoretical approximate formula would give about 14 percent. If one were to draw a final conclusion from these two results, it would have to be said: $\frac{dc_a}{d\alpha}$ is decreased by sweepback, but the decrease appears to be only about 60 percent of the theoretical value. (When swept-back wings are constructed in the usual manner according to which the profile, and in particular its percentage thickness $\frac{d}{t}$ is given in the direction of the wind, then c_a' really should have another correction because the profile sections in the direction of the effective flow incidence - that is, perpendicular to the one-quarter chord line - have a different thickness than the prescribed profile.) According to Ringleb (12) $c_a'_\infty$ when sweep angle is used changes by the factor $k = \cos\varphi + 0.723 \frac{d}{t}(1 - \cos\varphi)$ where the first term is due to the changed thickness. Since this influence is already contemplated in our calculation, c_a' should be multiplied by the factor $1 + 0.723 \frac{d}{t}\left(\frac{1}{\cos\varphi} - 1\right)$. For a thickness of 12 percent this means for $\varphi = 30°$ an increase of c_a' by 1.3 percent and an increase of 3.6 percent for $\varphi = 45°$.

While the above discussed question of the total lift is perhaps practically not so important, the practical engineer is especially interested in the form of the lift distribution on swept-back wings, especially because of its

importance for the position of the neutral point, and for the behavior of the wing with respect to flow separation. From the experimental side this question may only be completely answered by pressure-distribution measurements. To date, these have only been made by Luetgebrune who measured a trapezoidal wing with $\varphi = 0^\circ$ and with $\varphi = \pm 35^\circ$. The lift distributions obtained do not reveal any notable influence of sweepback at all. (This fact, however, may be due to the circumstance that the measurement was carried out on a wing-half with end plate at the center of the wing, so that the behavior at the center of the wing, precisely where the greatest effect of sweepback is to be expected theoretically, might have been falsified.)

From the balance measurements only one intergrated value is to be taken, namely the position of the neutral point on the wing chord, or for $\varphi \neq 0$ the spanwise position of the center of lift of a wing-half. In this way the general impression, based on experiments, that the neutral point may be determined from the lift distribution of the unswept-back wing if $\varphi < 15^\circ$, is confirmed by theory, since a deviation of 1/2 percent of the average wing chord would be difficult to detect experimentally. For $\varphi = 30^\circ$ Kuhle (5) found in the NACA measurements a difference of 17 percent of the average wing chord between calculation and experiment; this enormous difference is due to a mistake in calculations, but the Multhopp evaluation of this measurement does show a comparatively great influence of sweepback on the position of the center of lift, which for the most part agrees quite well with the results of this calculation. However, one must bear in mind that for the experimental determination of the center of lift (in its dependence on), it is not the distance of the measured neutral point from the quarter-chord line (which is its theoretical position at $\varphi = 0$) but rather its distance from the neutral point measured at $\varphi = 0$ which is of consequence. Then one gets, using $\frac{\Lambda}{2} = 3$, from table VI (1) the following values for the position $\frac{ab}{2}$ of the center of lift:

$$\varphi = 15^\circ: \quad a = \frac{0.022 + 0.352}{3 \tan \varphi} = 0.465$$

$$\varphi = 30^\circ: \quad a = \frac{0.022 + 0.775}{3 \tan \varphi} = 0.460$$

That is, the center of lift, according to this, actually is displaced somewhat toward the center of the wing, as the sweepback increases. The Blenk wings showed the same behavior: no increase in a in going from $\varphi = 15^\circ$ to $\varphi = 30^\circ$, rather, a small decrease. If one assumes that the experimental value of a determined for $\varphi = 15^\circ$ is also approximately correct for $\varphi = 0^\circ$, which may very well be the case, there are, especially for $\varphi = 0^\circ$, great differences between theory and experiment.

a at $\varphi = 0^\circ$	Theory		Experiment
	L-method	Multhopp	
Rectangle $\Lambda = 5$	0.439	0.451	0.475
Trapezoid $\Lambda = 6$, $z = 2$	.424	.430	.465

As a matter of fact, pressure-distribution measurements show that the actual lift distribution near the wing tips is greater than the theoretical, which may be explained by the influence of tip vortices. Hansen (4) gives no neutral-point positions, probably on account of the rather nonlinear variation of $c_m(c_a)$. It may, however, be determined here also that the Multhopp method for $\varphi = 40^\circ$ gives too great a displacement.

In summary it may be said that the Multhopp method gives too large values for the displacement of the neutral point, and the same is probably also true for the F-method and the L-method, since experiments up to $\varphi = 30^\circ$ apparently show no influence of sweepback whatever on the center-of-lift position. Presumably this behavior may be explained by assuming that the boundary layer, following the pressure gradients of the swept-back wing, flows from the middle toward the wing tips where it is piled up by the oppositely directed flow about the wing tips. The presence of such flow in the boundary layer may be clearly seen from flow pictures (tufts, and coloring matter in the water tunnel) made by Hansen. Another indication that the differences between theory and experiment are to be sought in boundary-layer influences is the fact that the influence of the Reynold's number on $c_a(\alpha)$, $c_m(c_a)$, and $c_{a_{max}}$ is considerably greater for swept-back wings than for straight wings.

Finally, a few remarks about wings without sweepback. With reference to the form of the lift distribution, the new methods may be expected to give not better agreement with measured lift distributions, but rather a somewhat poorer agreement; for while the difference between the old and the new distributions for large aspect ratio consists in a decrease of the lift, especially at the wing tips, the experimental distributions at the tips already give values too large (compare the note on p. 22). Since this effect clearly has the character of nonlinearity with respect to α it will not be comprehended by any linear theory of the lifting surface, no matter how accurate.

The difference between the theoretical and experimental values of c_a' has hitherto been explained by saying that, even for the wing with infinite aspect ratio, c_a' could be expected to be less than the theoretical value. This hypothesis is only conditionally true, as is shown by a glance at figure 13. In this figure the calculated values of c_a' according to the $\overline{F}$-method, and by the Prandtl lifting-line theory using $c'_{a\infty} = 2\pi$ are plotted versus the aspect ratio Λ, together with some experimental values obtained with very thin wings, which agree very well with the c'_{aF} curve. According to this, there is no boundary-layer effect present for very thin profiles, $c'_{a\infty}$ is equal to the theoretical value 2π, and the differences obtained hitherto are due solely to failure to take into account the influence of the surface effects. Naturally even here, especially for small aspect ratios, a perfect agreement between experiment and lifting-surface theory is not to be expected on account of the tip effects. In addition, for normal wings, there is the influence of profile thickness, which according to the plane theory should have as a result an increase of $c'_{a\infty}$ while experiment shows a decrease. It is this effect which may probably be correctly attributed to the boundary layer.

In this connection a method for calculating c_m similar to the F-method would appear to be desirable, since the relation between c_m and c_a can be tested directly by experiment. Since the induced velocity on the surface increases from the leading edge toward the rear, a displacement of the neutral point from the one-quarter chord line forward is to be expected with decreasing aspect ratio, and this is in harmony with experience.

IV. NOTE ON THE SWEPT-BACK WING IN YAW

The formula for the rolling moment due to yaw is given incorrectly in almost all of the pertinent literature, the argument being: the lift of a straight wing is decreased in yaw by $\cos^2\beta$ from which the change for the two halves of a swept-back wing in yaw is $\cos^2(\varphi - \beta)$ for the advancing wing half, and $\cos^2(\varphi + \beta)$ for the lagging half. If A is the total lift, and if we assume the center of lift of a wing half at $\frac{b}{4}$, the rolling moment due to sideslip will be

$$L = \frac{A}{2}\frac{b}{4}\left[\cos^2(\varphi - \beta) - \cos^2(\varphi + \beta)\right] = \frac{Ab}{8}\sin 2\varphi \sin 2\beta$$

The error in this derivation lies in the false analogy between the straight wing in yaw, and the swept-back wing. If a straight wing is put in yaw, both the normal and tangential components are decreased by $\cos\beta$ so that the lift takes on a factor of $\cos^2\beta$. But if a straight wing is given sweepback, only the effective tangential component is changed by $\cos\varphi$ while the normal component remains unchanged, so that the lift is only to be multiplied by $\cos\varphi$. If now the swept-back wing is yawed, the normal components on both wing-halves change by $\cos\beta \approx 1$ and the tangential components take on the factors $\cos(\varphi - \beta)$ and $\cos(\varphi + \beta)$. Accordingly the correct rolling moment due to sideslip is

$$L = \frac{Ab}{8}\left[\cos(\varphi - \beta) - \cos(\varphi + \beta)\right] = \frac{Ab}{4}\sin\varphi \sin\beta \qquad (39)$$

$$C_L = \frac{L}{\frac{\rho}{2}V^2 F\frac{b}{2}} = \frac{C_a}{2}\sin\varphi \sin\beta \qquad (40)$$

while the old formula gives twice this amount. Tracing down this error in the literature is further complicated by the circumstance that the rolling moment is not always made dimensionless with $\frac{Fb}{2}$ as in this report, but with Fb instead.

So for instance, in the much used summary by Schlichting (13) there is a formula for C_L for small φ and β which is formally the same result as in equation (40). Nevertheless the Schlichting formula contains the above error since Fb was used in nondimensionalizing.

The only work known to me which avoid the above fallacy is Multhopp's paper (10), but since the error, even here, is not expressly emphasized, and rolling moment due to sideslip is only given in the form of an integral to be evaluated in every individual case over a lift distribution which has to be calculated for this case, the Multhopp results have been less noticed than some others. In addition, Multhopp is concerned with the oblique position of the free vortex sheet, which causes an additional angle of attack distribution $\Delta\alpha = \alpha_i \beta \tan\varphi$ where α_i is the induced angle of attack distribution for nonoblique flow incidence; the positive sign is to be taken for the advancing wing, and the negative for the retarded wing. While now, according to Multhopp, the lift distribution belonging to $\Delta\alpha$ must be calculated, and from it the corresponding rolling moment due to sideslip, one may by a somewhat cruder procedure obtain also in this case a closed formula.

To this end we assume the lift distribution of the wing without yaw to be approximately elliptical. Then α_i is constant along the span, and equal to $\frac{c_\alpha}{\pi\Lambda}$ likewise the absolute value of $\Delta\alpha$ is constant along the whole span, but the sign changes at the center from plus to minus. The lift distribution corresponding to a discontinuous distribution of α like this, is, for a wing half, approximately like the usual lift distribution of a wing of half the span. That is, the total lift coefficient associated with the $\Delta\alpha$ of a wing half, if we use the elliptical conversion formula, and $c'_{a\infty} = 2\pi$ is given by

$$2\pi \cos\varphi \frac{\frac{\Lambda}{2}}{\frac{\Lambda}{2}+2} \Delta\alpha = \pm\pi\beta \sin\varphi \frac{\Lambda}{\frac{\Lambda}{2}+2} \alpha_i = \pm\beta \sin\varphi \frac{2c_a}{\Lambda+4} \qquad (41)$$

From this we get for the coefficient of the corresponding rolling moment:

$$\beta \sin\varphi \frac{c_a}{\Lambda + 4}$$

Together with the moment (40) of the bound vortices, this gives for the total rolling moment due to yaw resulting from sweepback the convenient formula

$$\frac{\partial c_L}{\partial \beta} = c_a\left(0.5 + \frac{1}{\Lambda + 4}\right) \sin\varphi \qquad (42)$$

V. SUMMARY

Two methods have been developed for calculating the lift distribution over the span, which takes into account the influence of the distribution of the circulation over an area better than the Prandtl lifting-line theory, and which may both be used on wings with sweepback. For swept-back wings, the first method, called the F-method, is numerically very laborious, and therefore, serves only as a check of the simpler L-method. The check is very good, even at large sweep angles. The computations for a straight wing require about 3 hours, for the swept-back wing, about 8 hours. A series of examples was calculated numerically, from which the following conclusions may be drawn:

1. For the straight wing the new method gives a noticeable decrease of c'_a when compared with the Prandtl method, which for example at $\Lambda = 5$ amounts to about 8 percent. If the profile is very thin, the experimental values seem to lie very well on the new c'_a curve. According to this, the difference between the old lifting-line theory and experiment, in the case of very thin profiles, is not to be attributed to a decrease of the theoretical $c'_{a_\infty} = 2\pi$ because of boundary layer, but comes from neglecting the two-dimensional distribution of the circulation.

2. In figure 4 the ratio $\frac{c'_a F}{c'_a P}$ of the new c'_a to the old is plotted versus the aspect ratio Λ. Since the curve is pretty flat in the interval of normal aspect ratios, the conversion formulas for changing from one aspect ratio to another are not essentially changed. The curve may, however, be used for correcting the rolling moments caused by antisymmetrical angle of attack distributions. For this purpose, one would have to multiply the moment calculated by the old theory by the value of $\frac{c'_a F}{c'_a P}$ scaled off of the curve at the point $\frac{\Lambda}{2}$. Thus for example one would get for the rolling moment due to sideslip resulting from dihedral a decrease of 15 percent while measurement gives 18 percent. This is for a rectangular wing with aspect ratio of 5.

3. For swept-back wings a comparison of the L-method with the method of Multhopp (10) was carried out. The L-method gives a greater decrease of c'_a and a smaller displacement of the neutral point caused by sweepback than the Multhopp method; moreover, it converges more rapidly.

4. Available experiments show less change of c'_a caused by sweepback than predicted by the L-method, and either no displacement at all or very small displacement of the center of load in the spanwise direction. These differences between theory and experiment are presumably to be explained by a movement of boundary-layer material toward the wing tips, and this is verified by flow observations.

5. The formula customarily given for the rolling moment due to sideslip of the bound vortices of a swept-back wing rests on a fallacy, and gives values which are 100 percent too large. In section IV a convenient closed formula is derived for the rolling moment due to yaw resulting from sweepback, in which formula the influence of the free vortices is also taken into account.

Translation by H. R. Grummann
McDonnell Aircraft Corporation

VI. BIBLIOGRAPHY

1. R. F. Anderson: Determination of the Characteristics of Tapered Wings. NACA Rep. 572 (1936).

2. H. Blenk: The Monoplane as a Lifting Surface of Vortices. Z. angew. Math. Mech. Vol. V (1925), p. 36.

3. H. Blenk: Göttingen Six-Component Measurements of Wings with Dihedral, Sweepback, and Twist. Luftf. - Forschg. Vol. 3 (1929), p. 27.

4. W. Hansen: Wings of Constant Chord with Sweepback and Twist in Yaw. FB 1411.

5. E. Kuhle: Calculation of the Neutral Points of Wings. Luftf. - Forschg., Vol. 17 (1940), p. 257.

6. H. Luetgebrune: Contributions to Swept-Back Wing Theory. FB 1458.

7. H. Luetgebrune: Pressure Distribution Measurements on Swept-Back Wings. FB 1501.

8. E. Moeller: Six-Component Measurements of Rectangular Wings with Dihedral, and Sweepback in a large interval of Yaw Angle. Luftf. - Forschg. Vol. 18 (1941), p. 243.

9. H. Multhopp: The Calculation of Lift Distribution of Wings. Luftf. - Forschg. Vol. 15 (1938), p. 153.

10. H. Multhopp: The Application of Airfoil Theory to Questions of Flight Mechanics. Ref. 5-2 of the Lilienthal Society for Aeronautical Research, p. 53.

11. E. Pistolesi: Considerations Respecting the Mutual Influence of Systems of Airfoils. Collected Lectures of the 1937 Principal Meeting of the Lilienthal Society, Berlin (1937).

12. F. Ringleb: Some Aerodynamical Relations for the Wing with Oblique Flow Incidence. FB 1497.

13. H. Schlichting: Recent Contributions of Research to the Aerodynamic Design of Wings. 1940 Yearbook of German Aeronautical Research. p.I 113.

14. J. Weissinger: The Wing in Yaw and Unstalled Flow. 1940 Yearbook of the German Aeronautical Research. p. I 145.

15. H. Winter: Flow Phenomena on Plates and Profiled Bodies of Small Span. Forschg. auf d. Gebiete d. Ingenieurwesens, Vol. 6 (1935) Edition A. p. 40,67.

16. K. Wieghardt: On the Lift Distribution of the Simple Rectangular Wing along the Chord. Z. angew. Math. Mech. Vol. 19 (1939), p. 257.

SUPPLEMENT

In comparing my evaluation of the VDT measurement with the Multhopp evaluation ((10) fig. 3), I could not find the point corresponding to the wing 24-15-0. Writing to Mr. Multhopp about this, I was informed that he had omitted this point because he did not think it was correct. At the same time he sent me the accompanying amplified diagram in which there is, in addition, a new point 1.

This figure seems at first to verify the correctness of the Multhopp calculation, this also if one only considers the inclination of the theoretical straight line. In my report only wings 5 and 7 were used, because these were the only ones for which nothing was changed but the angle of sweepback in starting from $\varphi = 0^{\circ}$; for all other wings the profile and the twist were changed at the same time, for no. 1 even the plan form was changed. The thesis that sweepback causes no essential displacement of center of lift is thus confirmed by the only comparable measurements 5 and 7 (and by Blenk (3)). Against this conclusion may be adduced the other measurements, as well as the fact that by extrapolation to $\varphi = 0^{\circ}$ one obtains centers of lift located very far out. (The allusion in my report to tip effect may not be sufficient as an explanation as Multhopp correctly remarks.) Finally, if one considers that the calculation of a from measurements of c_m rests on the assumption that the neutral points of the individual profile sections are not changed by sweepback, one must probably say in conclusion that a final answer to the question cannot yet be given on the basis of the experimental results available at the present time.

TABLE I

μ at M = 7	μ at M = 15	μ at M = 31	n = 1	n = 2	n = 3	n = 4
0	0	0	2.6131	-1.4142	1.0824	-0.5000
-	-	1	4.5889	-2.1053	1.5663	-.7193
-	1	2	2.8844	-.2363	+.0751	-.0253
-	-	3	.6573	2.0046	-1.5402	.7109
1	2	4	-1.4142	3.6955	-2.4142	1.0824
-	-	5	-2.7625	4.1506	-2.0037	.8553
-	3	6	-3.1207	3.1958	-.3621	.1005
-	-	7	-2.5843	1.2224	1.8601	-.8209
2	4	8	-1.5307	-1.0000	3.6955	-1.4142
-	-	9	-.4383	-2.6609	4.2950	-1.2844
-	5	10	.3114	-3.2465	3.3216	-.3367
-	-	11	.5651	-2.7288	1.1207	1.1492
3	6	12	.4142	-1.5307	-1.4142	2.6131
-	-	13	.1016	-.2939	-3.2260	3.4397
-	7	14	-.1258	.4372	-3.5579	3.2212
-	-	15	-.1444	.4635	-2.2904	1.9416

The numbers $F_{n\mu}$ at m = 7.

TABLE II

μ	n = 1	n = 2	n = 3	n = 4	n = 5	n = 6	n = 7	n = 8
0	5.1258	-2.6131	1.8000	-1.4142	1.2027	-1.0824	1.0196	-0.5000
1	-2.6131	6.9258	-4.0273	3.0027	-2.4966	2.2223	-2.0824	1.0196
2	-3.3258	-1.4142	6.3285	-3.6955	2.8196	-2.4142	2.2223	-1.0824
3	1.1989	-3.9231	-1.0824	6.1454	-3.6131	2.8196	-2.4966	1.2027
4	-.5973	1.5307	-4.1062	-1.0000	6.1454	-3.6955	3.0027	-1.4142
5	.3318	-.7804	1.6131	-4.1062	-1.0824	6.3285	-4.0273	1.8000
6	-.1831	.4142	-.7804	1.5307	-3.9231	-1.4142	6.9258	-2.6131
7	.0824	-.1831	.3318	-.5973	1.1989	-3.3258	-2.6131	5.1258

The numbers $T_{n\mu}$ at m = M = 15

TABLE III

μ at M = 7	μ at M = 15	μ at M = 31	ν = 1	ν = 2	ν = 3	ν = 4
0	0	0	-0.0761	-0.2929	-0.6173	-1.0000
-	1	2	-.0569	-.2737	-.5981	-.9808
1	2	4	0	-.2168	-.5412	-.9239
-	3	6	.0924	-.1244	-.4488	-.8315
2	4	8	.2168	0	-.3244	-.7071
-	5	10	.3683	.1515	-.1729	-.5556
3	6	12	.5412	.3244	0	-.3827
-	7	14	.7288	.5120	.1876	-.1951
4	8	16	.9239	.7071	.3827	0
-	9	18	1.1190	.9022	.5778	.1951
5	10	20	1.3066	1.0898	.7654	.3827
-	11	22	1.4794	1.2627	.9382	.5556
6	12	24	1.6310	1.4142	1.0898	.7071
-	13	26	1.7554	1.5386	1.2142	.8315
7	14	28	1.8478	1.6310	1.3066	.9239
-	15	30	1.9047	1.6879	1.3635	.9808
8	16	32	1.9239	1.7071	1.3827	1.0000

The differences $\cos\phi_\nu - \cos\phi_\mu$ at m = 7

CONTINUATION OF TABLE III

μ at M = 15	υ = 1	υ = 2	υ = 3	υ = 4
1	-0.0713	-0.2881	-0.6125	-0.9952
3	-.0330	-.2498	-.5742	-.9569
5	.0420	-.1748	-.4992	-.8819
7	.1509	-.0659	-.3903	-.7730
9	.2895	.0727	-.2517	-.6344
11	.5066	.2898	-.0346	-.4173
13	.6336	.4168	.0924	-.2903
15	.8259	.6091	.2847	-.0980
17	1.0219	.8051	.4807	.0980
19	1.2142	.9974	.6730	.2903
21	1.3412	1.1244	.8000	.4173
23	1.5583	1.3415	1.0171	.6344
25	1.6969	1.4801	1.1557	.7730
27	1.8058	1.5890	1.2646	.8819
29	1.8808	1.6640	1.3396	.9569
31	1.9191	1.7023	1.3779	.9952

TABLE IV

μ	$\upsilon = 1$	$\upsilon = 2$	$\upsilon = 3$	$\upsilon = 4$	$\upsilon = 5$	$\upsilon = 6$	$\upsilon = 7$	$\upsilon = 8$
0	-0.0192	-0.0761	-0.1685	-0.2929	-0.4444	-0.6173	-0.8049	-1.0000
1	0	-.0569	-.1493	-.2737	-.4252	-.5981	-.7857	-.9808
2	.0569	0	-.0924	-.2168	-.3683	-.5412	-.7288	-.9239
3	.1493	.0924	0	-.1244	-.2759	-.4488	-.6364	-.8315
4	.2737	.2168	.1244	0	-.1515	-.3244	-.5120	-.7071
5	.4252	.3683	.2759	.1515	0	-.1729	-.3605	-.5556
6	.5981	.5412	.4488	.3244	.1729	0	-.1876	-.3827
7	.7857	.7288	.6364	.5120	.3605	.1876	0	-.1951
8	.9808	.9239	.8315	.7071	.5556	.3827	.1951	0
9	1.1759	1.1190	1.0266	.9022	.7507	.5778	.3902	.1951
10	1.3635	1.3066	1.2142	1.0898	.9382	.7654	.5778	.3827
11	1.5364	1.4794	1.3870	1.2627	1.1111	.9382	.7507	.5556
12	1.6879	1.6310	1.5386	1.4142	1.2627	1.0898	.9022	.7071
13	1.8123	1.7554	1.6629	1.5386	1.3870	1.2142	1.0266	.8315
14	1.9047	1.8478	1.7554	1.6310	1.4794	1.3066	1.1190	.9239
15	1.9616	1.9047	1.8123	1.6879	1.5364	1.3635	1.1759	.9808
16	1.9808	1.9239	1.8315	1.7071	1.5556	1.3827	1.1951	1.0000

The differences $\cos\phi_\upsilon - \cos\phi_\mu$ at $m = M = 15$

TABLE V

	Rectangle $\Lambda = 5$		Trapezoid $\Lambda = 5$ $z = 2$		$\Lambda = 5$
φ°	c'_a	$\Delta c'_a$ in percent	c'_a	$\Delta c'_a$ in percent	$\frac{\varphi^2}{2}\frac{100\Lambda}{\Lambda+2}$
0	3.92	0	4.06	0	0
15	3.79	-3.1	3.98	-2.0	2.5
30	3.49	-10.7	3.72	-8.5	9.8
45	2.99	-23.6	3.22	-21.0	22.0

The coefficient c'_a as a function of the swept-back angle (according to the L-method)

TABLE VI

Calculation of a		With Multhopps squaring formula									Graphical		
Method		Multhopp K = 1, m = 7			F-method			L-method			L-method		
Wing	φ°	a	Δa	$\frac{\Lambda}{2}$ Δa tan φ	a	Δa	$\frac{\Lambda}{2}$ Δa tan φ	a	Δa	$\frac{\Lambda}{2}$ Δa tan φ	a	Δa	$\frac{\Lambda}{2}$ Δa tan φ
	0	0.451	0	0	0.440	0	0	0.439	0	0	0.438	0	0
Λ = 5	15				.451	.011	.007	.450	.011	.007			
	30							.463	.024	.035			
Z = 1	45	.505	.054	.135	.483	.043	.107	.481	.042	.105	.472	.034	.085
	0	.429	0	0				.424	0	0	.423	0	0
Λ = 5	15							.433	.009	.006			
	30							.443	.019	.027	.440	.017	.025
Z = 2	45	.485	.056	.140				.457	.033	.082	.450	.027	.068
Λ = 6	0	.430						.424					
Z = 2	30							.447	.023	.040			
Λ = 10	0	.431						.427					
Z = 2	45							.472	.045	.225			

NATIONAL ADVISORY
COMMITTEE FOR AERONAUTICS

The distance a from the plane of symmetry of the lift center of gravity of a wing half in terms of semispan.

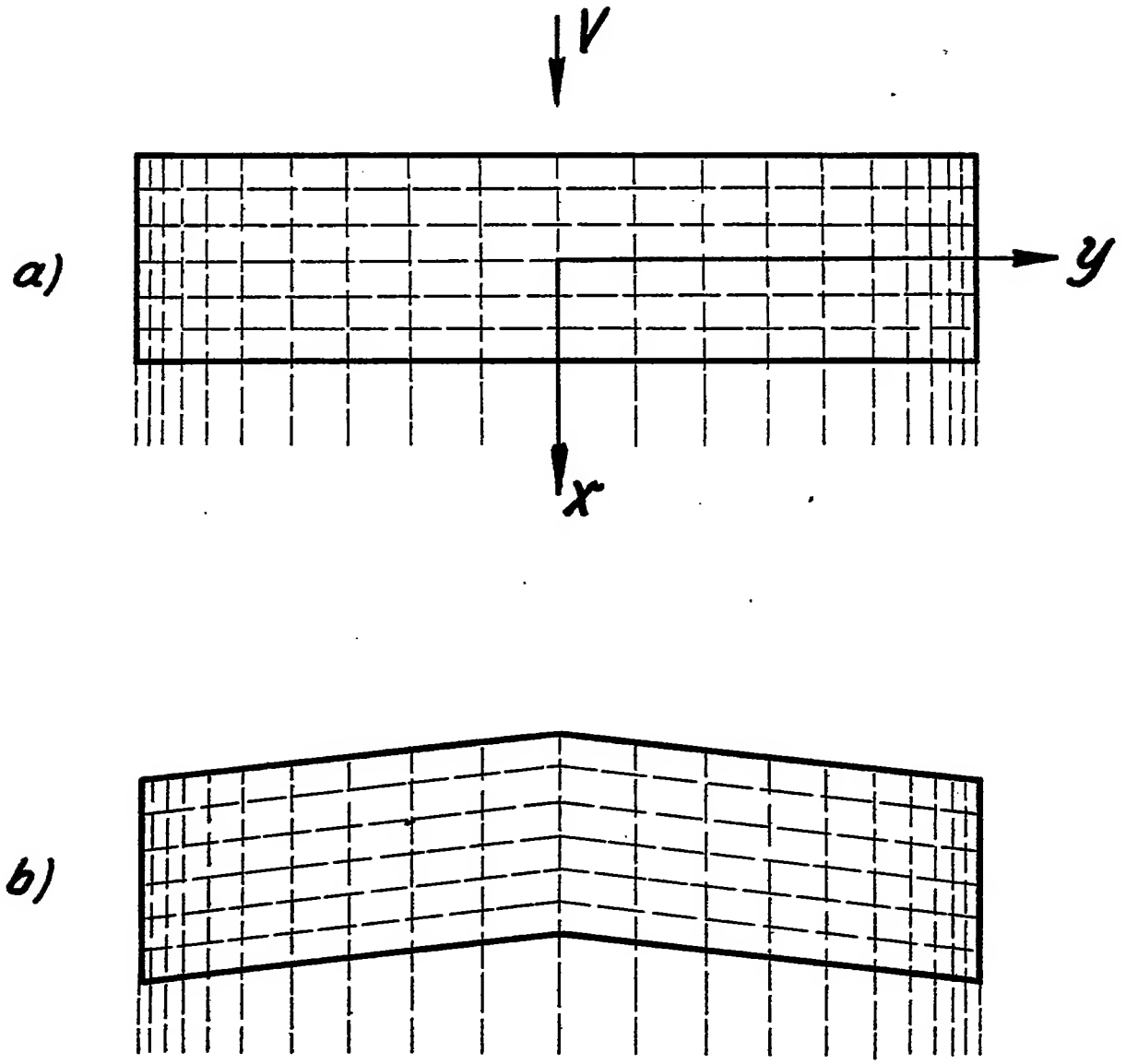

Figure 1. The vortex system of the lifting surface

(a) Straight-rectangular wing

(b) Swept-back rectangular wing

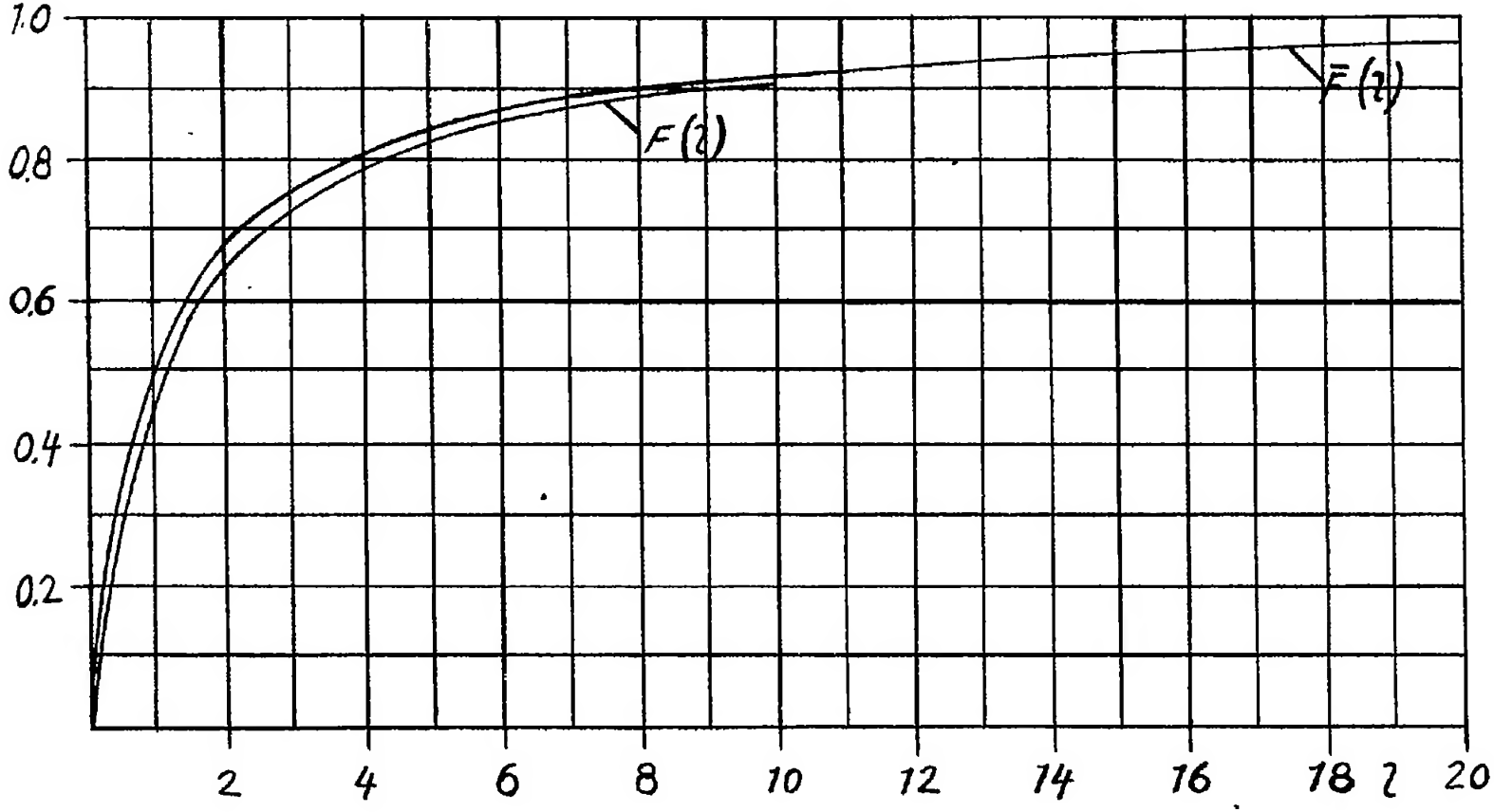

Figure 2. The functions F (l) and $\bar{F}$ (l)

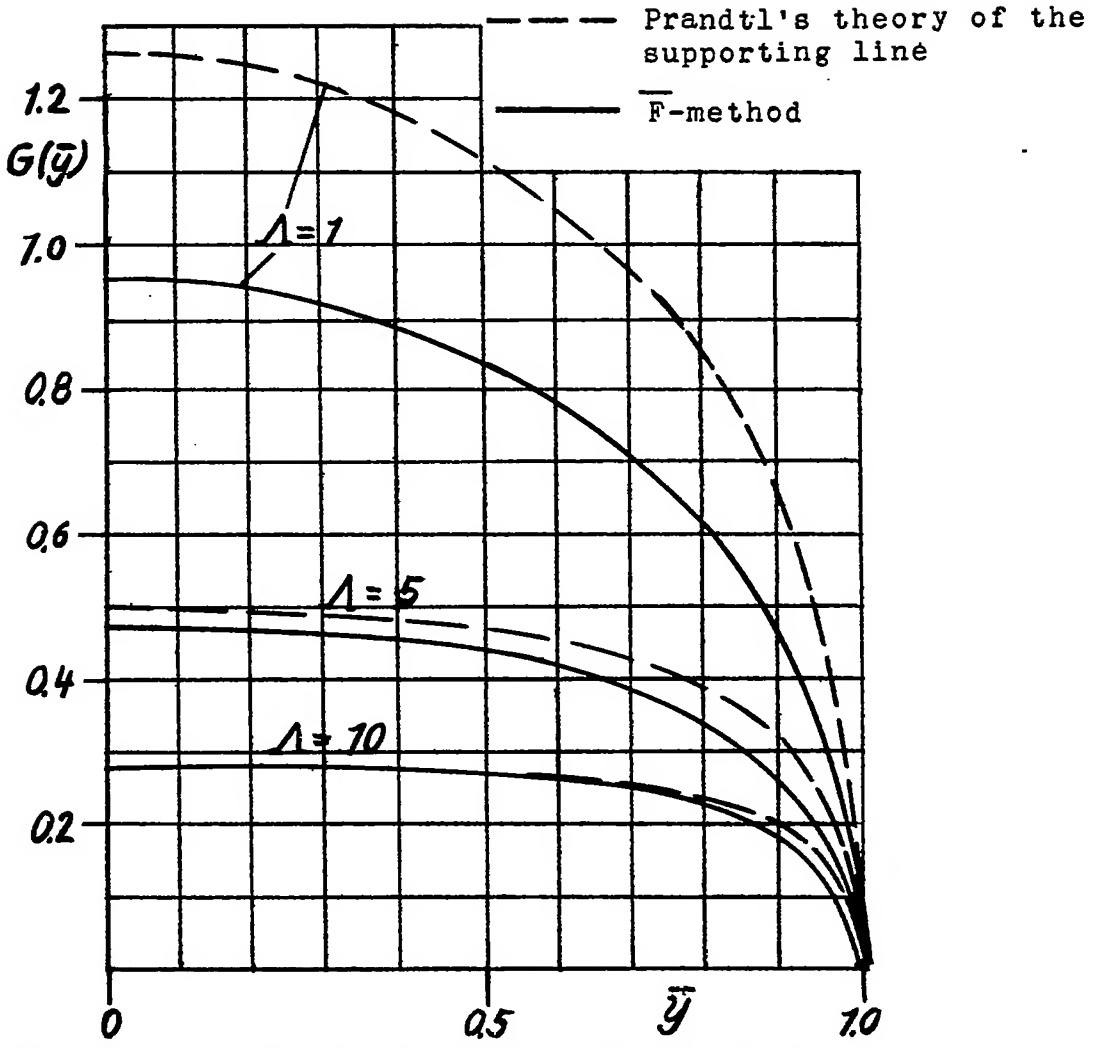

Figure 3. Lift distribution of the 3 rectangular wings = 1, 5, 10, Comparison of Prandtl's theory of the supporting line with the lifting surface method.

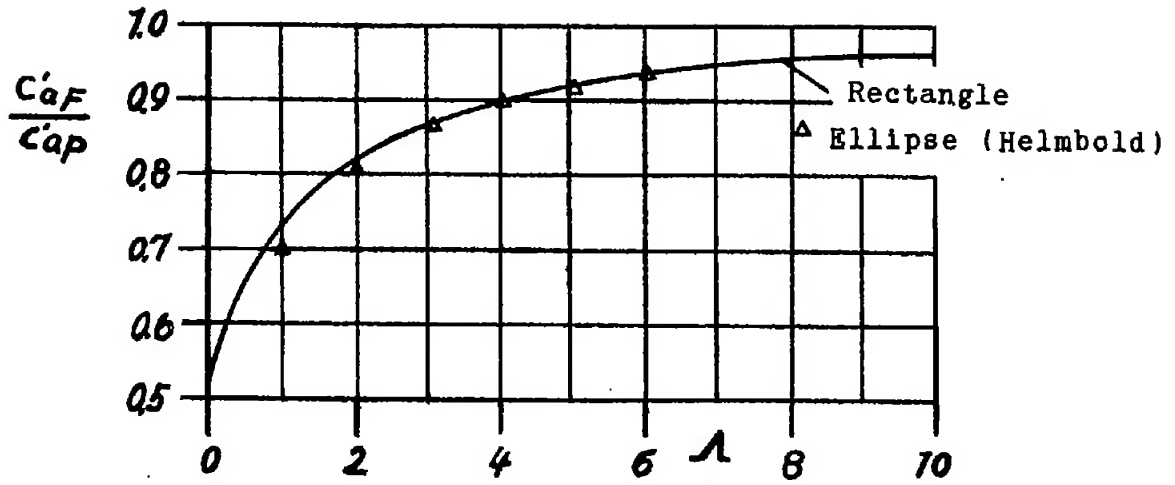

Figure 4. The relation $\frac{C_{aF}}{C_{ap}} = \frac{C_{aF}}{C_{ap}}$ for rectangular wings of the ratios $0 \div 10$ (C_{a_F} = lift coefficient according to the $\overline{F}$-method, C_{a_p} = lift coefficient according to Prandtl's theory of the supporting line with $C_{a_m} = 2\pi$).

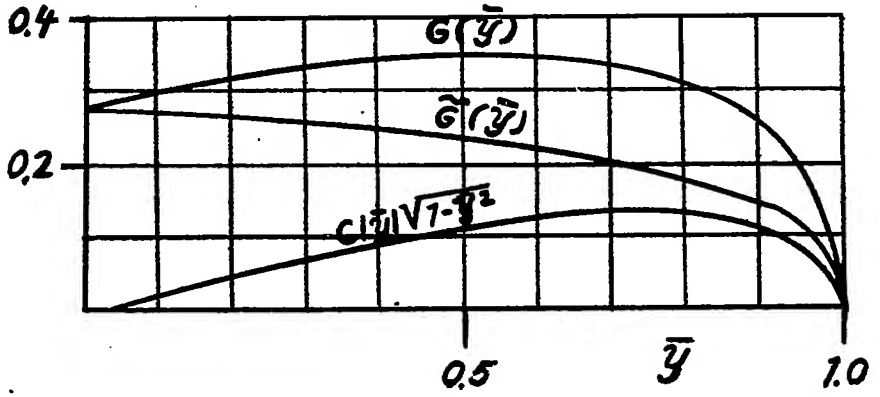

Figure 5. The lift distribution G ($\bar{Y}$) of the 45° rectangular swept-back wing $\Lambda = 5$ as the sum of 2 distriburions $\tilde{G}$ ($\bar{Y}$) and C ($\bar{Y}$)$\sqrt{1-\bar{Y}^2}$ (F-method).

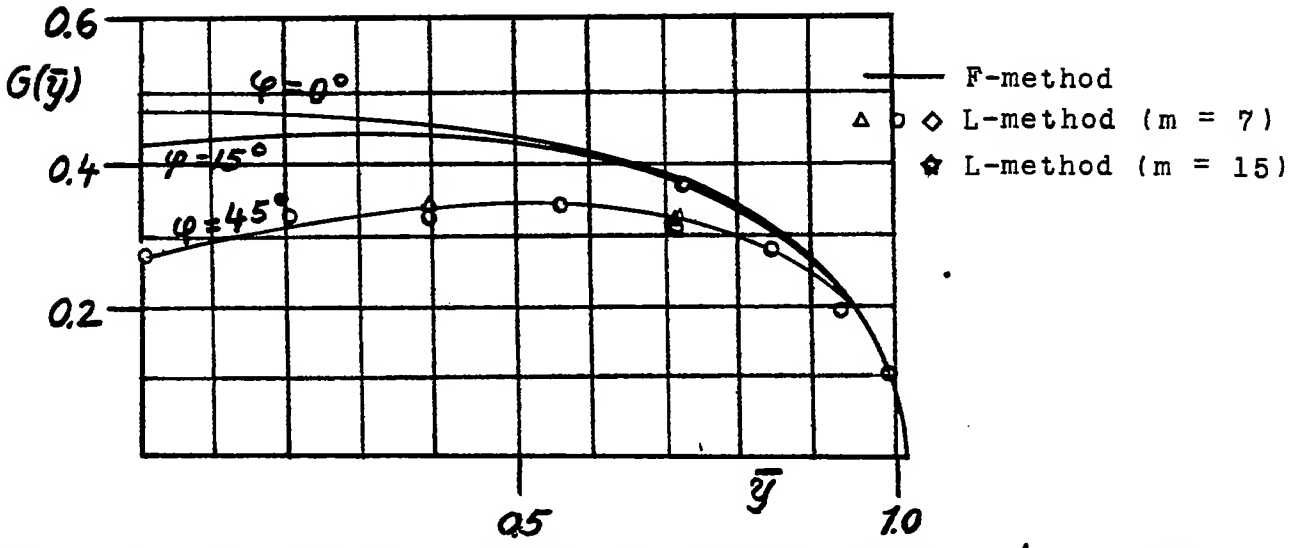

Figure 6. Lift distributions of the rectangular wing $\Lambda = 5$ with the sweep-back angles $\varphi = 0°$, 15° and 45° according to the lifting surface and supporting line method.

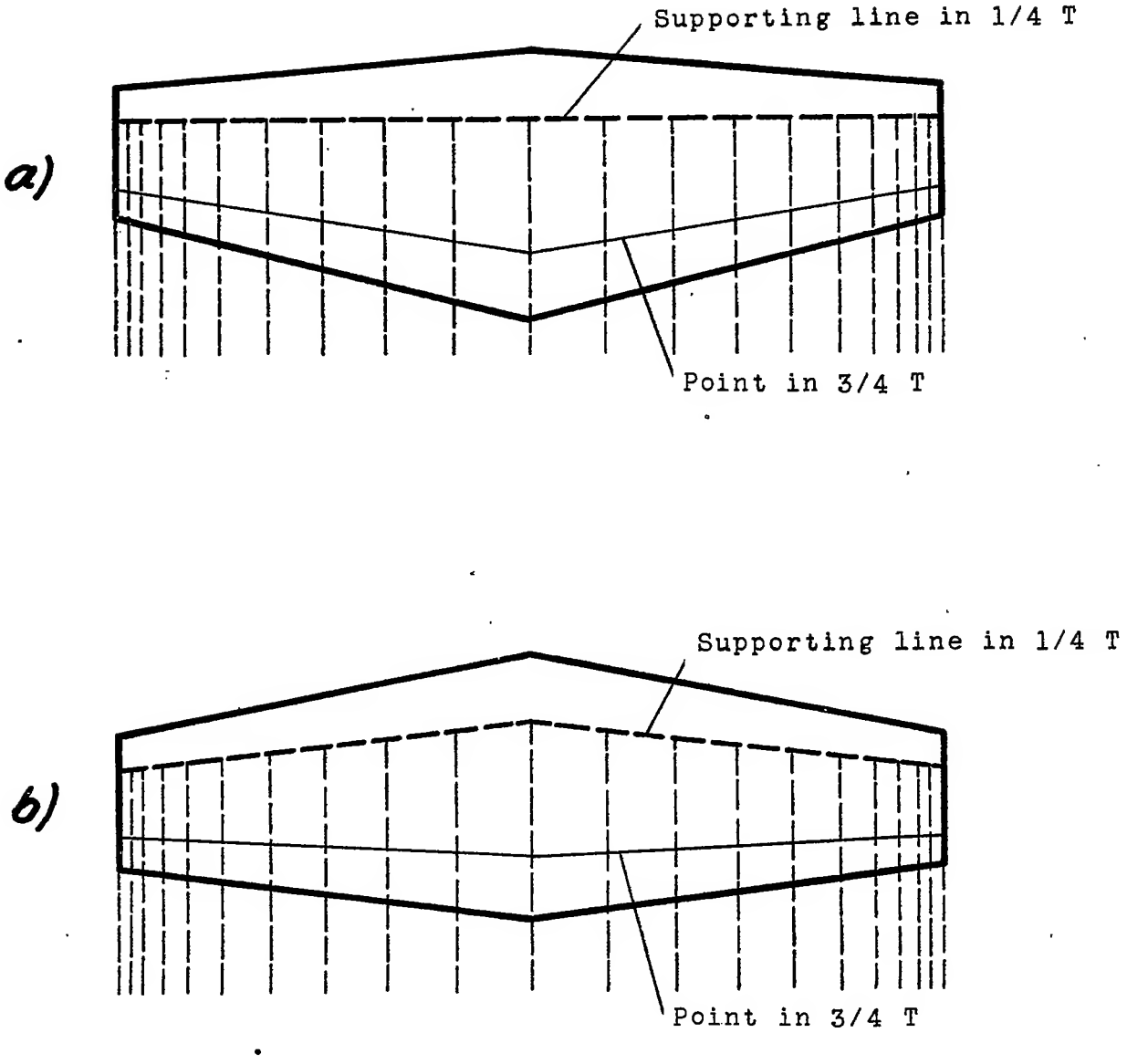

Figure 7. The vortex model of the L-method

(a) Wing without sweep back

(b) Swept-back wing

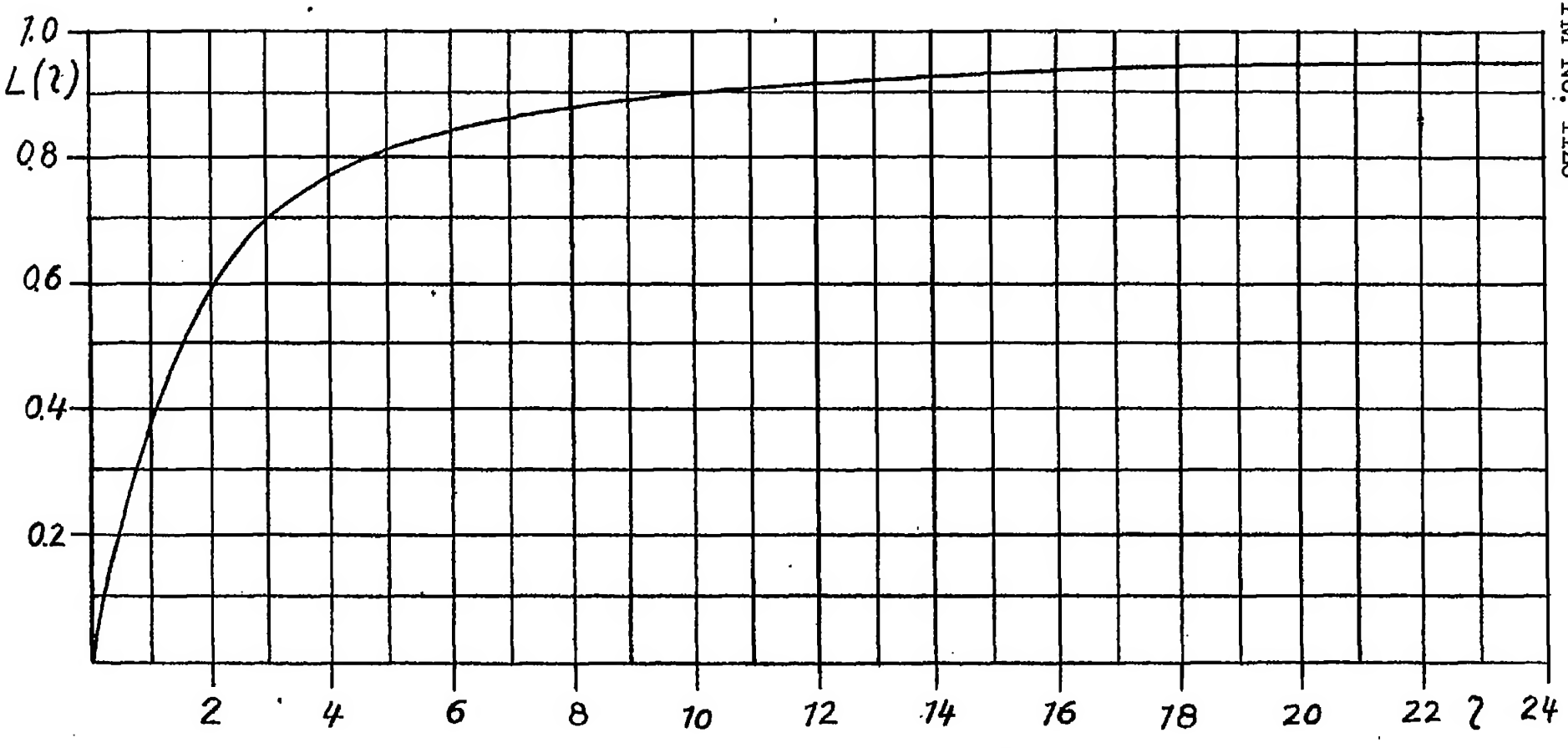

Figure 8. The function $L(l)$

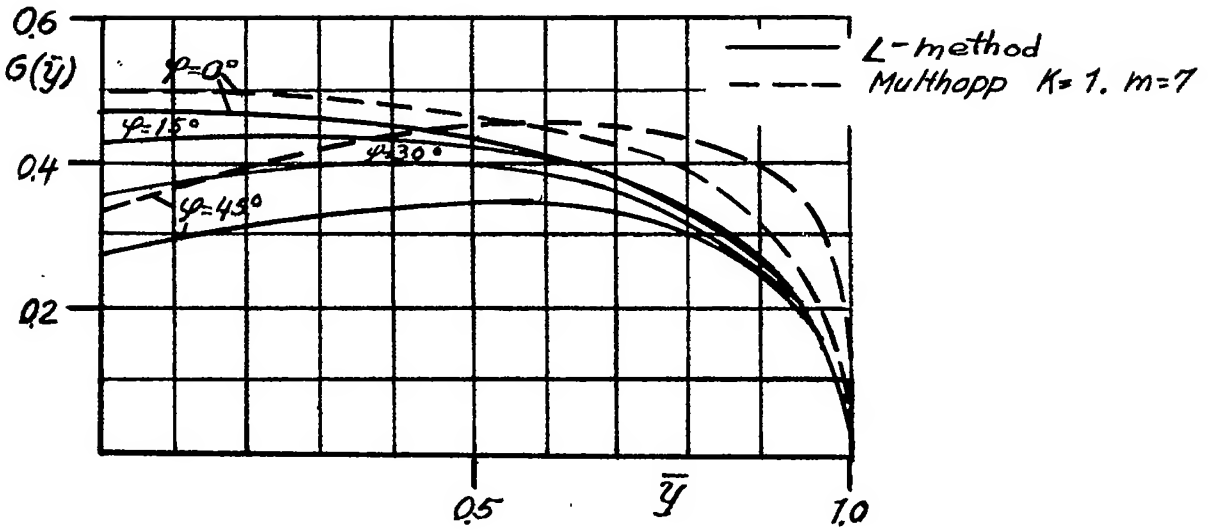

Figure 9. Lift distributions of the rectangular wing $\Lambda = 5$ with the swept-back angles $\varphi = 0°$, 15°, 30° and 45°, according to the L-method. Dashed line; result of Multhopp's method for (K = 1, m = 7) for $\varphi = 0°$ and 45°.

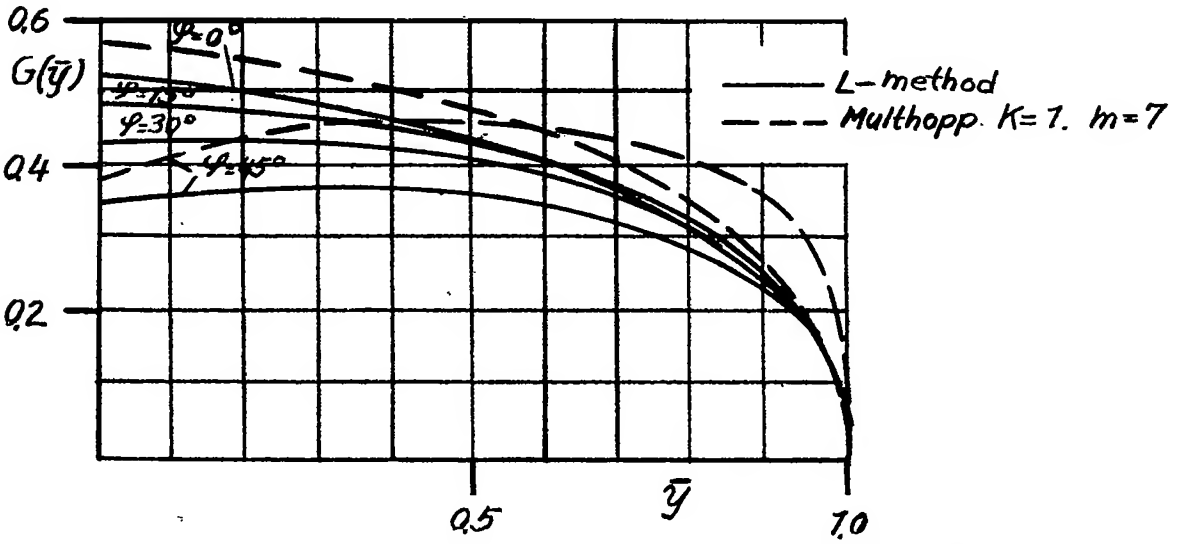

Figure 10. Lift distributions of the trapezoidal wings, $\Lambda = 5$, $\mathbf{Z} = 2$ with the swept-back angles $\varphi = 0°$, 15°, 30° and 45°, according to the L-method. Dashed line; result of Multhopp's method for ; (K = 1, m = 7) for $\varphi = 0°$ and 45°.

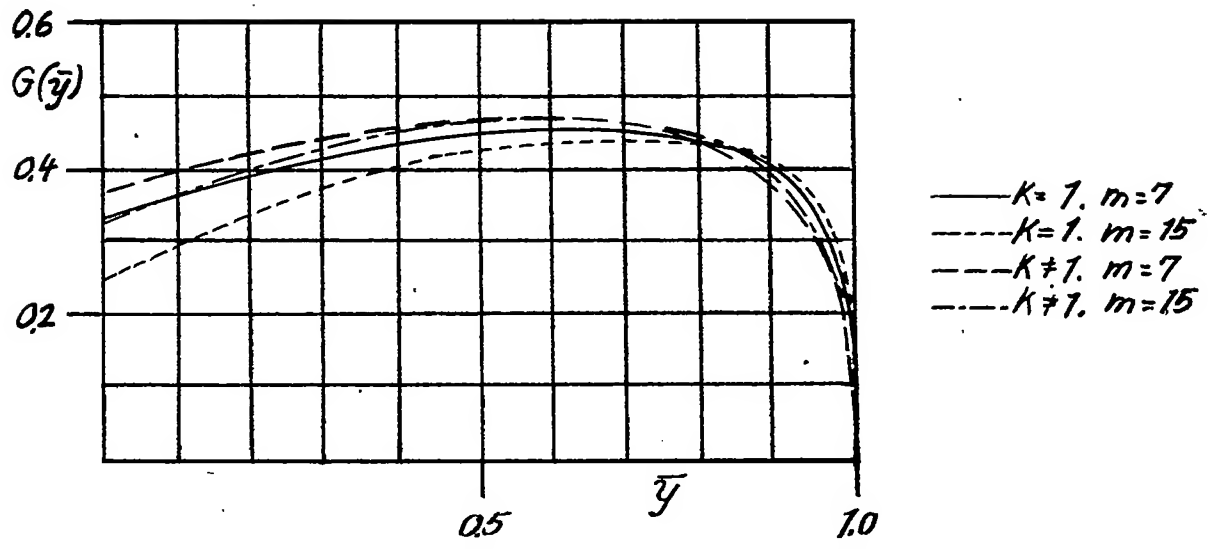

Figure 11. The converging of Multhopp's method for the rectangular wing; $\Lambda = 5, \varphi = 45^{\circ}$.

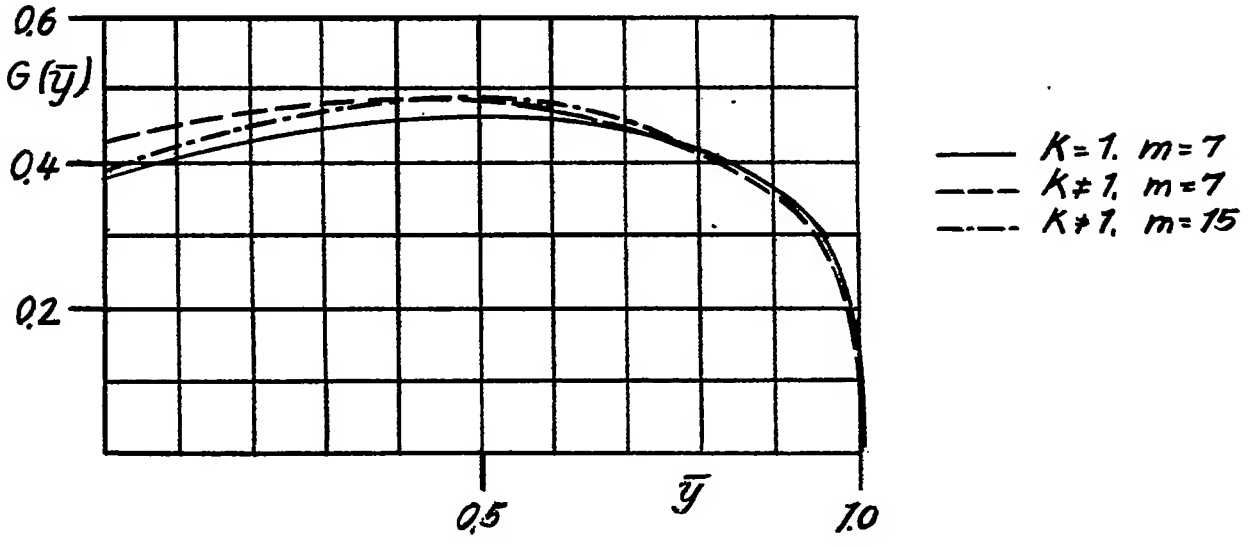

Figure 12. The converging of Multhopp's method for the trapezoidel wing; $\Lambda = 5$, $\lambda = 2, \varphi = 45^{\circ}$.

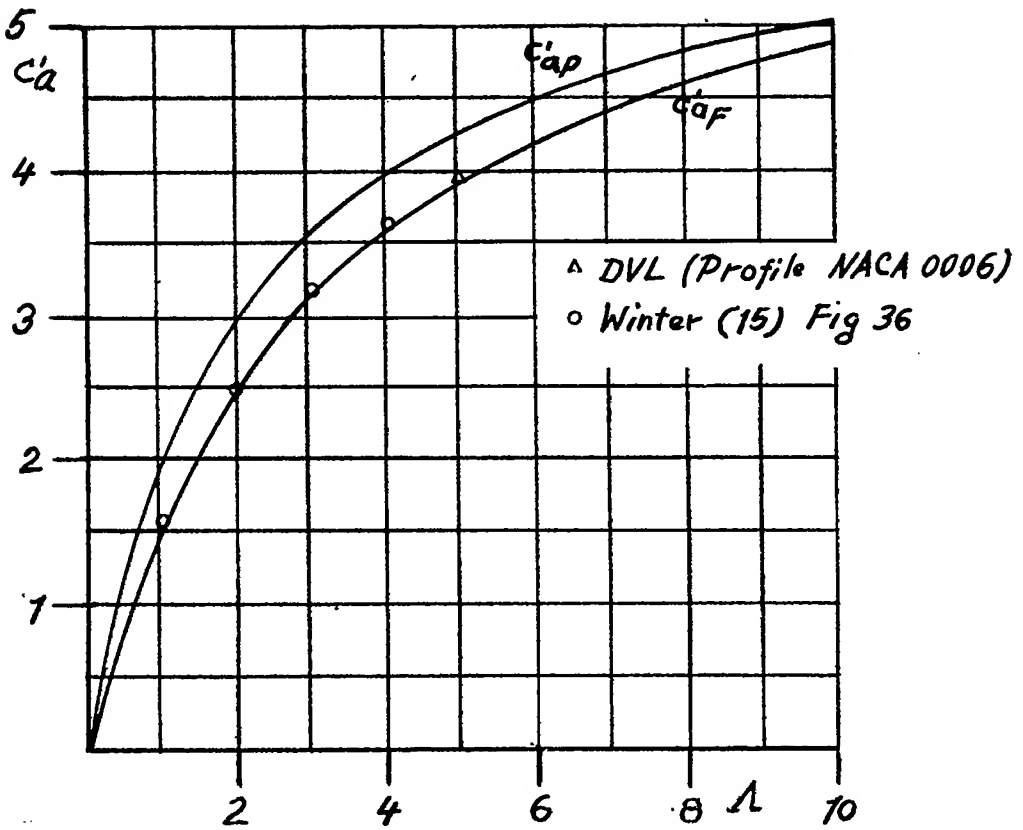

Figure 13. The coefficients C'_{aF} ($\bar{F}$-method) and C'_{ap} (Prandtl's theory of the supporting one $C'_{a\infty} = 2\pi$) compared with measurements on very thin profiles.